GEODERMA

Estimating the mass wetness of Spanish arid soils from lightness measurements

M. Sánchez-Marañón[a,*], R. Ortega[b], I. Miralles[a], M. Soriano[b]

[a] *Dpto. Edafología y Química Agrícola, Facultad de Ciencias, Universidad de Granada, 18071 Granada, Spain*

[b] *Dpto. Edafología y Química Agrícola, CITE II-B, Universidad de Almería, 04120 Almería, Spain*

* Corresponding author. *E-mail address*: msm@ugr.es

Abstract

The colour of a soil changes with its water content. This paper investigates the ability of spectrophotometric colour measurement to predict soil mass wetness (w). We looked at the CIELAB parameters (L^*, C^*_{ab}, h_{ab}) and spectral profile of 76 A soil-horizons from south-eastern Spain to (i) group them by colour, (ii) calibrate within each group the relationships between water content and colour in disturbed and undisturbed samples, and (iii) test the validity of predictive models. Four groups of differently coloured soils were selected from the reflectance curves. Models constructed only with L^* (lightness) from the dryness state to the water content at -33/-10 kPa explained the greatest variation in w (R^2= 0.77-0.97), regardless of the soil colour or sample type. The decrease in soil lightness with increasing water content was noted mainly at -1500 kPa, -400/-100 kPa, and -33/-10 kPa potentials. At intermediate potentials, however, L^* did not strongly correlate with w, especially in undisturbed samples, which showed a greater colour variability. Although the predictive models did not give estimates of w with high enough precision (mean relative errors 25.3-56.6%), the measured values below -1500 kPa, between -1500 and -100 kPa, and above -100 kPa were predicted within the same interval of water potential. The results indicate that predictions of the dryness condition, presence of plant-available water and wetness near to field capacity, but not the specific water content, can be made with reasonable confidence in any soil by using the models calibrated in other soil of similar colour.

Keywords: soil colour, water retention, regression model, spectrophotometer.

1. Introduction

Water content on a mass or volume basis and water potential affect plant growth, root respiration, microorganism activity, the chemical state of the soil, swelling and shrinking processes, and such mechanical properties as consistency, plasticity, strength, compactability, penetrability, stickiness, and trafficability (Hillel, 2004; Lal and Shukla, 2004). Unfortunately, the methods to measure water content and potential (Dane and Topp, 2002), both independently as well as through the soil-moisture characteristic curve require highly specialized equipment and are costly and time-consuming. For these and other reasons (e.g., the use of the already available soil data) attempts have been made to predict soil-water-retention data from more easily determined soil properties (Rawls et al., 1991).

Several models and classification schemes are available in the literature for estimating soil-water characteristics from texture, bulk density, mineralogical composition, organic-matter content and structure (Ahuja et al., 1985; De Jong and Mckeague, 1987; Mecke et al., 2002; Vaz et al., 2005). Soil colour is today routinely measured in field and laboratory; however, the relationship between moisture and colour has not yet been appropriately modelled despite the potential application of spectroscopy for soil-moisture measurements (Chang et al., 2005; Mouazen et al., 2007). The assumption that colour can be used to estimate soil water, also indicated by Rawls et al. (1991), is supported by the results of De Jong et al. (1983), who used organic matter and texture data to construct separate water-retention equations depending on soil colour.

The colour of most soils changes between 1/2 and 3 Munsell value steps according to water content (Baumgardner et al., 1985; Soil Survey Division Staff, 1993). This is a consequence of the increase in refractive index of material surrounding the soil particles. Upon wetting, air (refractive index n = 1) is replaced by water, which has a refractive index (n = 1.33) closer to that of the soil particles (n = 1.40-1.70). Light scattering decreases as the difference in refractive index between particles and their surrounding medium decrease (Berns, 2000). As a result, a very large amount of light should be absorbed when soil is wet, thereby decreasing soil lightness (Munsell value, CIE luminance or CIELAB L^*).

On chernozemic soils, Shields et al. (1968) noted a lower Munsell value with higher soil-moisture content. More recently, Barrett (2002), moistening samples from spodic sandy soils also reported a homothetic reduction in reflectance across all the visible wavelengths and, consequently, a decrease in CIELAB L^*. Hue (CIELAB h_{ab}) and chroma (CIELAB C^*_{ab}) showed an irregular behaviour. Bedidi et al. (1992) observed opposite results in ferralitic soils: a non-uniform decrease in visible spectral reflectance, with the CIE dominant wavelength λ (hue) going towards the red and the CIE purity Pe (chroma) decreasing systematically at high moisture levels. The reason for this variable effect of water content on soil colour appears to be because of either (i) different colour-measurement conditions in their studies or (ii) different colorimetric behaviour depending of soil type. The silica lamella used by Bedidi et al. (1992) in their measurements led to variations of CIE luminance which were of the same order due to moistening. Bhadra and Bhavanarayana (1997) investigated the influence of soil type and found that the effect of soil moisture on colour is more or less the same for soils having similar dry colour. They suggested that grouping soils on a colour basis may be useful to estimate the water content of any soils grouped by regression equations.

Because the above-mentioned works dictate that samples have been disturbed and sieved at 2 mm, the applicability of laboratory findings to the field is unclear. In addition, only Bedidi et al. (1992) controlled the water potential. Therefore, the connection with the water-retention curve or pore-size distribution has not yet been amply studied. The present study was conducted to develop models for the regression of water content on colour parameters, calibrating the relationships in disturbed and undisturbed soil samples, with and without control of the water potential. We performed colorimetric prospecting in arid soils from Spain in order to select, on the one hand, soils in which to develop the models and, on the other, soils for testing the hypothesis that the models constructed can be used to predict the moisture of soils of similar colours.

2. Material and Methods

2.1. Spectrophotometer and colour parameters

Laboratory and field measurements of soil reflectance and colour were made using a portable Minolta CM-2600d spectrophotometer (Minolta, Osaka, Japan). This instrument has an integrating sphere of 52 mm of diameter with illuminating/viewing geometry d/8 and three pulsed xenon lamps as light sources. A silicon photodiode array detects the light reflected by the soil surface from 360 to 740 nm at 10-nm intervals with a repeatability of 0.1%. We selected the greatest measuring port available in the spectrophotometer (8-mm-diameter area circular) owing to the heterogeneity of soil samples, and the specular component excluded mode to avoid glistening.

From the spectral profile of colours, we recorded the CIELAB cylindrical polar coordinates h_{ab}, L^*, C^*_{ab} for D65 standard illuminant and CIE 1964 Standard Observer (CIE, 1986). The CIELAB h_{ab}, which, like Munsell hue, is given in a circular scale, starts with 0º for a red colour and increases to 90º for yellow, 180º for green, and 270º for blue. Both the CIELAB L^* and Munsell value represent the colour-perception attribute termed lightness, the former ranging from 0 to 100. Finally, CIELAB C^*_{ab}, like Munsell chroma, is the relative strength of a colour, C^*_{ab} being measured as the length of the segment from the neutral point to the sample point in a horizontal plane. Munsell and CIELAB parameters are well correlated but the latter are strongly recommended for numerical, statistical, or predictive analysis (Viscarra Rossel et al., 2006).

2.2. Site description and sampling

The study area was located at Tabernas Desert in southern Spain, between 2º 21‘ 32“ and 2º 38‘ 30“ W and between 36º 55‘ 39“ and 37º 10‘ 20“ N. This area contains badlands, pediments, residual erosion surfaces, and hills. The soils are mainly Regosols (IUSS Working Group WRB, 2006). The parent material consists of schists, phyllites, marls, sandstones, gypsum-calcareous mudstones, conglomerates and alluvial sediments. Altitude ranges from 140 m to 1231 m. Slope changes in topographic transects between 5 and 50%. The mean annual rainfall is 258 mm and mean annual temperature is 17.3 ºC. Moisture soil regimes are xeric and aridic, and the temperature regime is thermic.

A random field sampling with 76 points was performed to collect the variability of topsoil colours. At each point, a bulked sample of the A horizon was taken, air-dried, passed through a 2-mm sieve (fine earth), and placed in circular aluminium containers (diameter 15 mm, thick 4 mm) for colour measurements. Subsequently, four differently coloured A horizons were selected to test linear-regression models (S1-S4, Table 1) of water content on colour parameters, and 28 A horizons, grouped as G1-G4 (Table 2) according to their similarity in colour to S1-S4, were used to validate the models. At the sites of S1-S4, soil cores of 2493 cm^3 (diameter 23 cm, height 6 cm) and 115 cm^3 (diameter 7 cm, height 3 cm) preserving the original soil surface were manually removed from the topsoil with stainless-steel cylinders.

2.3. Determination of physical and chemical properties

Soil properties were analysed using the standard methods described by Page et al. (1982) and Klute (1986). The particle-size distribution was determined by sieving and the pipette method, soil-bulk density by the cylindrical-core method, and particle density with a pycnometer. The total porosity was estimated from the particle and bulk density, and macroporosity from total porosity less microporosity, the latter being measured as water content at -33 kPa. The pH (1:1) in water was determined by potentiometry, using the extracts to measure electrical conductivity. Cation-exchange capacity and exchangeable Ca^{2+}, Mg^{2+}, K^+, and Na^+ at pH 7.0 were determined by ammonium acetate extraction. We determined the organic C content by the dichromate oxidation method, the $CaCO_3$ content with a Bernard calcimeter, and the content of free Fe oxides by atomic absorption spectrophotometry in citrate–bicarbonate–dithionite extracts. Mineralogical analysis in the fine earth was performed by X-ray diffraction using a Philips Pw 1140 equipped with a nickel filter and Cu*K*α radiation.

2.4. Calibration curves for the regression models

We constructed four multiple linear-regression models from each test soil (S1-S4) using the forward stepwise analysis available in the statistical program Statgraphics (STSC Inc., Rockville, MD). The entry of variables into the models was controlled by an F-ratio criterion of 4 (Schabenberger and Pierce, 2002). Model 1 was prepared in order to take into account the natural wetting of soil. The 2493 cm^3 soil cores (protected by their steel rings) were air-dried and placed with their bottom on a fibreglass screen (Ø = 1 mm) superimposed over a metal screen (Ø = 10 mm), so that the soil could drain freely. Wetting the samples involved daily spraying of distilled water as a fine mist onto the soil surface to achieve successively greater moisture levels. Once saturated, soil cores were allowed to air-dry again. Water content and colour were measured in both the wetting and drying period, registering a total of between 17 and 22 moisture levels. At each level, 10 spectrophotometer readings were taken at different points on the surface and 3 sub-samples for determining soil mass wetness (w) by the oven-drying method (Hillel, 2004), their averages being used for regression analysis and their standard deviations for assessing variability.

Following the procedures described by Bhadra and Bharanarayana (1997) and Barrett (2002), spectrophotometric calibration curves were also constructed using fine-earth samples (Model 2). Ten moisture cans were prepared with approximately 40 g of fine earth and the necessary water content for achieving *w* close to: air dry, 2%, 4%, 6%, 8%, 10%, 15%, 20%, 25%, and 30%. After the soil and water were thoroughly mixed with a penknife, we replaced the lid of the cans and let the mixtures stand for 24 h at 4 °C. Then we took three sub-samples of each can for soil-colour measurement, placing the samples in circular aluminium containers (diameter 15 mm, thick 4 mm) and trimming the surfaces till flat. The water content determined in each can was regressed against the mean colour parameters.

Finally, we performed the procedure described by Bedidi et al. (1992) for relating water content and colour at several potentials. Desorption curves were measured by a pressure plate extractor (Soilmoisture Equipment Corp. Santa Barbara, CA) at potentials of *h* = -10, -33, -100, -400, -700, -1000 and -1500 kPa (Klute, 1986), using undisturbed 115 cm^3 soil cores (Model 3) and disturbed samples (Model 4), the latter being made of repacked fine earth within rubber retainer rings (diameter 6 cm, height 1.5 cm). On the porous plate of the pressure apparatus, three replicates of each soil sample were soaked in a shallow layer of water for 24 h. After equilibrium at a given potential for 48 h, spectrophotometric readings were taken at three surface points, then the water content was determined. Wetness and colour at saturation, air-dryness, and oven-dry at 105 °C for 24 h were also considered in the regression analysis.

2.5. Validation measurements

For the comparison of predicted and measured values of *w* in soils having a similar colour to that used for developing the model, we carried out field measurements on soils G1-G4, thus testing, respectively, the models constructed in S1-S4. On different dates, and therefore also with differing soil-moisture contents, we measured the spectrophotometric colour on unaltered soil surfaces (mean of 10 points) to validate Models 1 and 3, and on crushed and smoothed topsoil samples to validate Models 2 and 4. To measure *w*, we took samples from the uppermost 4 cm of the soil at the time of measuring the colour, then being transported to the laboratory in closed moisture cans, put into isothermal bags, and placed into the oven within two hours after collection.

3. Results and discussion

3.1. Grouping and selecting soils on a colour basis

The colour of 76 studied soils, as occurs in other arid and semiarid soils (Post et al., 1994), was influenced mainly by the geological substrate, most probably due to their low degree of weathering and incorporation of organic matter (ochric horizons). On the average, the colour difference (ΔE^*_{ab}, CIE, 1986) in our soils with and without organic matter, when removed by H_2O_2, was only 2.8 ± 2.0 CIELAB units, 61% of the total due to ΔL^*, 30% to ΔC^*_{ab}, and 9% to ΔH^*_{ab}. In contrast, Spielvogel et al. (2004) found a greater influence of organic matter in the colour of soils with a moderate pedogenetic development and mollic, umbric or histic horizons. Therefore, the soils of Tabernas Desert developed over schists proved significantly (analysis of variance, $P< 0.05$) darker and more achromatic ($L^* = 43.2 \pm 2.5$, $C^*_{ab} = 10.2 \pm 3.3$, n=15) than the badlands soils over mudstones and sandstones ($L^* = 54.6 \pm 4.5$, $C^*_{ab} = 17.1 \pm 3.8$, n=30), whereas the soils derived from conglomerates had a decidedly more reddish hue ($h_{ab} = 67.9 \pm 6.15$, n = 19). The colour proved uneven in the 12 remaining soils sampled over alluvials, phyllites and gypsums, and therefore were not considered for further analysis.

The value and shape of the reflectance curves for soils grouped by parent material (Fig. 1) enabled us to rule out soils of an anomalous colour or too light or dark with respect to the general trend of the group. The broken curves in Fig. 1a-c deviate from the general pattern of the respective soil-colour group, probably for excessive differences in soil composition, particle-size, or structure. Fig. 1b reflects the concomitance of the reflectance curves of type A, according to Orlov (1992), which correspond to light-brownish-grey colours (2.5Y 6/1.5), together with type-B curves of light-yellowish-brown soils (2.5Y 6/3). Consequently, two soil-colour groups were considered for the soils developed over mudstone and sandstone. Only the soils with reflectance curves drawn as solid lines in Fig. 1 were used for developing regression models (test soils S1-S4) and for assessing the applicability of these models in other soils of similar colour (validation soils G1-G4).

The resemblance between the moisture-characteristic curves for soils with very similar reflectance curves is clear in Fig. 2. On the contrary, the water content in fine earth at a number of fixed potentials increased from dark-grey soils (S1 and G1) to brown (S4 and G4), light-yellowish-brown (S3 and G3), and light-brownish-grey soils (S2 and G2). The most notable differences in water content were found at potentials between -10 kPa and -100 kPa, referred to as the textural pore region potential interval (Jarvis and Messing, 1995). In the dark-grey and brown soils, which had a sandy texture, siliceous mineral composition, and a greater proportion of large pores (Tables 1 and 2), the water storage was over half compared with the other soil groups. The water content at lower potentials, where the retention is primarily by absorption forces (Mecke et al., 2002), was striking in light-brownish-grey soils that had more than 50% of silt+clay and a considerable salt content, when judged by the electrical-conductivity values. Although the differences in water retention amongst soils were due to the components and properties, these differences appear to be well represented by the soil colour.

3.2. Linear-regression models

Table 3 lists the four multiple linear-regression models developed for each test soil (S1-S4). Most models include only one or two colour variables because of the presence of multicollinearity. The three colour parameters tend to decrease in value with moistening (Bedidi et al., 1992). Often, the stepwise regression included the C^*_{ab} and/or h_{ab} variables, despite that their value changed slightly with wetness as indicated by their ranges (Table 3).

On the contrary, L^*, which exhibited a dramatic change, was found to be insignificant or did not improve the performance of many of the models. On the other hand, the independent variables and coefficients of determination differed between models in an irregular way. For example, the relationship between chromaticity (C^*_{ab} and/or h_{ab}) and mass wetness (w) proved considerably more accurate in S1 than in S2, with particular contrast in the relation w - C^*_{ab} of Model 2 (R^2= 0.92 and 0.39, respectively). Also, the accuracy of the relationships in the four models of S3 varied between 0 and 0.94, and the colour variable that best predicted w in S4 differed according to the type of sample. The data indicate that from the lowest moisture to the wettest possible condition of a soil the relationships between water content and colour parameters are irregular, resulting in heterogeneous and inconsistent models.

For all the soils and sample types, there was a moisture threshold, above which the soil lightness (L^*) reversed its negative relationship with the mass wetness. Fig. 3 and 4 indicate the value of this threshold of around 12-15% for intact soil cores and between 10% (coarsest-textured sample) and 18% (finest-textured sample) for fine-earth samples, which in our potential data is closest to the water content at -33 kPa or -10 kPa, except for the fine earth of S3 (Fig. 4). According to the capillary equation (Hillel, 2004), these potentials correspond to 0.01-0.03 mm equivalent pore diameter, i.e. the limit between micropores and macropores (Luxmoore, 1981). Barrett (2002) cited a decrease in soil lightness in fine earth wetted up to 20% moisture, attributable to glistening. This occurs when the reflection is specular (Berns, 2000); given that in our experiment, we registered diffuse reflection, we posit that soil lightness diminished with mass wetness until all the pores smaller than 0.01-0.03 mm are filled with water.

When the measurements above the moisture threshold were excluded from the regression analyses (Table 4), the variables C^*_{ab} and h_{ab} had P-values greater 0.05 or did not increase substantially R^2 of the models. The mass wetness w was correlated with lightness L^* at R^2 between 0.77 and 0.97 (P< 0.01, SEE= 0.68-2.47%). The L^* range determined for a given soil is similar in Models 1 and 3, both corresponding to soil-core samples, as well as in Models 2 and 4 for fine-earth samples. These latter were systematically lighter (higher L^*) because of sample preparation (Torrent and Barrón, 1993). The results signify that the type of sample has more influence in the development of the model than the control or not of the water potential, and that differences in water content of ± 3%, once the soil is dry or moist (w range in Table 4), do not measurably alter soil lightness.

The models based on soil cores accounted for less variance than did the fine-earth models (Table 4). The greater variability of the measurements in soil cores, as indicated by the scattering of points and error bars shown in Fig. 3, is consistent with the lower precision of Models 1 and 3. In the calibration curves of Model 1, the average standard deviation for L^* across 10 different sites on a soil-core at a given moisture level proved to be 3.96 for S1, 3.04 for S2, 3.63 for S3, and 4.76 for S4 (additional analysis of the data points shown in Fig. 3), implying that only lightness changes greater than these mean values can be informative of changes in water content. In S4, for example, there were no statistical differences in L^* when the soil-water content was < 3.5% (L^* = 35-40), between 5% and 10% (L^* = 30-35), and > 10% (L^* = 25-30) (Fig. 5a). In addition, a certain hysteretic behaviour of lightness detected in S1 and S4 could have contributed to the scattering of data for Model 1 (Fig. 3). At a given water content, L^* of S1 and S4 tended to be slightly lighter when measured in the drying branch (triangles) than in the wetting branch (diamonds).

On the other hand, L^* and w changes were found especially pronounced at -1500 kPa, -400/-100 kPa and -33/-10 kPa potentials. At lower potentials of -1500 kPa (air- and oven-dried samples) and between -1500 kPa and -400/-100 kPa, the variables L^* and w did not appear to be strongly correlated, as illustrated in Fig. 5b. This stepped behaviour of the relation between L^* and w, which is also suggested in the scatter plots of Fig. 3, reduces the precision of the regression models, especially in the undisturbed samples, in which the colour variability also provoked certain irregularities such as illustrated for -100 kPa in Fig. 5b. The assumption that soil lightness falls markedly at certain potentials, with minor and sometimes irregular variations between these, is supported by the results of Barrett (2002), who did not find appreciable changes in L^* between 3% and 10% moisture of soil samples studied in the laboratory and between 1% and 7% in the field.

3.3. Model validation

Because the soils selected to validate the models are grouped by colour similarity, the CIELAB parameters within groups G1-G4, and especially h_{ab} and L^*, showed a low variation (Table 2). The coefficient of variation for L^* in the validation sites fluctuated only between 3.5 and 6.5% (1.86-3.51 CIELAB units). The minor variation in colour contrasts with the high variability in organic carbon, free iron, carbonates, and soluble salts; this indicates that the contents in these components affect colour little, thus suggesting again that colour was essentially lithogenic. The colorimetric selection of the validation soils also enabled the variation range of soil properties in G1, G2, G3 and G4 to cover the values in the respective test soils S1, S2, S3 and S4 (Table 2). Special similarities were found in colour parameters, texture, porosity, and mineral composition.

With Models 1-4 of each test soil (Table 4) applied to the corresponding validation site, predicted and measured mass-wetness values were all significantly correlated ($P < 0.05$). However, there was considerable scatter in the data (Fig. 6). The mean differences between predicted and measured values (Table 5), which ranged between 1.17 and 3.05, represent a mean relative error of between 25.3% and 56.6%. The predictions were especially erroneous by using Models 1 and 3 (undisturbed cores) of the achromatic soils (G1 and G2). These errors are high in comparison with the good validation found for the models having textural and structural soil properties (De Jong and Mckeage, 1987; Mecke et al., 2002), and lowered the expectations of Bhadra and Bhavanarayana (1997) for using a single calibration curve to estimate the moisture of a group of soils with a similar colour. Nevertheless, it should be taken into account that the textural and structural approaches calculate water content separately at specific potentials, while the prediction equations developed in our work from soil lightness apply from dry soil to soil beginning to drain water.

The scatter of our predictions along the line 1:1 shows “low”, “intermediate”, and “high” values (Fig. 6), which appear to be related to two questions already shown in the test soils S1-S4: (i) the absence of significant differences of L^* within w ranges such as 0% - 3/5%, 3/5% - 8/10%, and 8/10% - 12/15%, and (ii) the abrupt transitions in the lowering of L^* with w at -1500 kPa and -400/-100 kPa. When we grouped the points for which the measured and predicted wetness corresponds to a potential lower than -1500 kPa, between -1500 kPa and -100 kPa, and greater than -100 kPa, according to the values registered in the corresponding test soil, only a few points remained isolated, signifying that the prediction is more satisfactory when considering these three wetness ranges. The dryness condition below the permanent wilting point (only residual pores < 0.2 μm can be filled by water retained at < -1500 kPa), the presence of plant-available water in the storage pores smaller than 3 μm (< -100 kPa), and the water near to field capacity were predicted reasonably well with either model at all the validation sites.

On the average, L^* changed from one wetness range to another at 6.4 ± 2.7 CIELAB units for undisturbed soil-surface, and at 8.5 ± 3.4 units for crushed and smoothed soil. These differences, which imply more than 0.5 steps of Munsell value (Viscarra Rossel et al., 2006), are visible according to the suprathreshold colour differences reported for surface colours (CIE, 1995). Therefore, for practical purposes, field guidelines based on soil lightness and calibrated against measured values could be used for visually estimating the mass wetness of soils with a similar origin and colour. The changes will be perceived somewhat better in crushed and smoothed soil, simplifying and controlling complex hydrological processes, which is one of the priorities to combat desertification in arid and semiarid region (Kosmas et al., 2006).

4. Conclusions

In the arid Regosols studied, hue-angle h_{ab} and chroma C^*_{ab} varied slightly and irregularly with the soil mass wetness (w) while soil lightness (L^*) decreased between 11.4 and 20.1 CIELAB units from dry to wet soil at -33/-10 kPa. Once the micropores were filled with water, L^* was maintained or slightly increased again with additional moistening. There was also multicollinearity between colour variables. Accordingly, the models constructed with L^* from dryness to near field capacity, proved more consistent and homogenous (R^2 = 0.77-0.97 SEE = 0.68-2.47%). The three most important L^* changes occurred at -1500 kPa, -400/-100 kPa, and -33/-10 kPa. Within wetness interval "low" (< -1500 kPa), "intermediate" (between -1500 and -400/-100 kPa), and "high" (> -400/-100 kPa), the variables w and L^* were not strongly correlated, especially in undisturbed soil cores because of the variability of L^* measurement (standard deviation = 3.04-4.76 units). For this reason the degrees of explanation for models constructed with undisturbed cores were somewhat lower than those of the fine earth.

Despite the high accuracy of the models for estimating soil mass wetness from soil lightness, when these were used in other soils located around the same area and with similar spectral-reflectance features to those in which models were constructed, the mean absolute and relative errors between measured and predicted values were, respectively, greater-than 1.17±0.83 and 25.3±24.4. This implies that the relationship between lightness and wetness was so soil-specific that the models could not be generally applied. Only estimates of "low", "intermediate", or "high" water content, considering the values at -1500 kPa and -100 kPa potentials as limits, can be made with reasonable confidence. Because measured and predicted data for most samples were fitted within these wetness ranges and the mean ΔL^* between two ranges is > 6.4 CIELAB units, visual estimations of the soil water condition could be made from soil-lightness guidelines calibrated below the permanent wilting point, with available water, and near field capacity.

Acknowledgements

Critical reviews by two anonymous reviewers and A.B. McBratney were very helpful in improving the presentation of our work. This work was financially supported by the Ministerio de Educación y Ciencia, Spain, through Project CGL2004-02282BTE.

References

Ahuja, L., Naney, J., Williams, R., 1985. Estimating soil water characteristics from simpler properties or limited data. Soil Science Society of America Journal 49, 1100-1105.

Barrett, L.R., 2002. Spectrophotometric color measurement in situ in well drained sandy soils. Geoderma 108, 49-77.

Berns, R.S., 2000. Billmeyer and Saltzman's Principles of Color Technology. John Wiley & Sons, New York.

Bhadra S.K., Bhavanarayana, M., 1997. Estimation of the influence of soil moisture on soil colour. Zeitschrift für Pflanzenernährung und Bodenkunde 160, 401-405.

Baumgardner, M.F., Silva, L.F., Biehl, L.L., Stoner, E.R., 1985. Reflectance properties of soils. Advances in Agronomy 38, 1-44.

Bedidi, A., Cervelle, B., Madeira, J., Pouget, M., 1992. Moisture effects on visible spectral characteristics of lateritic soils. Soil Science 153, 129-141.

Chang, G.W., Laird, D.A., Hurburgh, G.R., 2005. Influence of soil moisture on near-infrared reflectance spectroscopic measurement of soil properties. Soil Science 170, 244-255.

Commission Internationale de l'Éclairage (CIE), 1986. Colorimetry. CIE Central Bureau, Vienna.

Commission Internationale de l'Éclairage (CIE), 1995. Industrial colour-difference evaluation. CIE Central Bureau, Vienna.

Dane, J.H., Topp, G.C., 2002. Methods of Soil Analysis, Part 4: Physical Methods. Soil Science Society of America, Madison, WI.

De Jong, R., Campbell, C.A., Nicholaichuk, W., 1983. Water retention equations and their relationship to soil organic matter and particle size distribution for disturbed samples. Canadian Journal of Soil Science 63, 291-302.

De Jong, R., McKeague, J.A., 1987. A comparison of measured and modelled soil water retention data. Canadian Journal of Soil Science 67, 697-703.

Hillel, D., 2004. Introduction to Environmental Soil Physics. Elsevier, Amsterdam.

IUSS Working Group WRB, 2006. World reference base for soil resources 2006. World Soil Resources Reports No. 103. FAO, Rome.

Jarvis, N.J., Messing, I., 1995. Near-saturated hydraulic conductivity in soils of contrasting texture measured by tension infiltrometers. Soil Science Society of America Journal 59, 27-34.

Klute, A., 1986. Methods of Soil Analysis: Part 1, Physical and Mineralogical Methods, 2nd edn. American Society of Agronomy, Madison, WI.

Kosmas, C., Tsara, M., Moustakas, N., Kosma, D., Yassoglou, N., 2006. Environmentally sensitive areas and indicators of Desertification. In: Kepner, W.G., Rubio, J.L., Mouat, D.A., Pedrazzini, F. (Eds.), Desertification in the Mediterranean Region. A Security Issue. Springer, Dordrecht, pp. 527-547.

Lal, R., Shukla, M.K., 2004. Principles of Soil Physics. Marcel Dekker, New York.

Luxmoore, R.J., 1981. Micro-, meso-, and macroporosity of soil. Soil Science Society of America Journal 45, 671-672.

Mecke, M., Westman, C.J., Ilvesniemi, M., 2002. Water retention capacity in coarse podzol profiles predicted from measured soil properties. Soil Science Society of America Journal 66, 1-11.

Mouazen, A.M., Maleki, M.R., De Baerdemaeker, J., Ramon, H., 2007. On-line measurement of some selected soil properties using a VIS-NIR sensor. Soil and Tillage Research 93, 13-27.

Orlov, D.S., 1992. Soil Chemistry. Russian translations series, 92. A.A. Balkema Publishers, Brookfield, IL.

Page, A.L., Miller, R.H., Keeney, D.R., 1982. Methods of Soil Analysis: Part 2, Chemical and Microbiological Properties, 2nd edn. American Society of Agronomy, Madison, WI.

Post, D.F., Horvath, E.H., Lucas, W.M., White, S.A., Ehasz, M.J., Batchily, A.K., 1994. Relations between soil color and Landsat reflectance on semiarid rangelands. Soil Science Society of America Journal 58, 1809-1816.

Rawls, W.J., Gish, T.J., Brakensiek, D.L., 1991. Estimating soil water retention from soil physical properties and characteristics. Advances in Soil Science 16, 213-234.

Schabenberger, O., Pierce, F.J., 2002. Contemporary Statistical Models for Plant and Soil Sciences. CRC Press, Washington, DC.

Shields, J.A., Paul, E.A., St. Arnaud, R.J., Head, W.K., 1968. Spectrophotometric measurement of soil color and its relationship to moisture and organic matter. Candian Journal of Soil Science 48, 271-280.

Soil Survey Division Staff, 1993. Soil Survey Manual. Agricultural Handbook 18. US Government Printing Office, Washington, DC.

Spielvogel, S., Knicker, H., Kögel-Knabner, I., 2004. Soil organic matter composition and soil lightness. Journal of Plant Nutrition and Soil Science 167, 545-555.

Torrent, J., Barrón, V., 1993. Laboratory measurement of soil color: theory and practise. In: Bigham, J.M., Ciolkosz, E.J. (Eds), Soil Color. Soil Science Society of America, Madison, WI, pp. 21-33.

Vaz, C.M.P., de Freitas Iossi, M., de Mendonça Naime, J., Macebo, A., Reichert J.M., Cooper, M., 2005. Validation of the Arya and Paris water retention model for Brazilian soils. Soil Science Society of America Journal 69, 577-583.

Viscarra Rossel, R.A., Minasny, B., Roudier, P., McBratney, A.B., 2006. Colour space models for soil science. Geoderma 133, 320-337.

Fig. 1. Reflectance curves for soils developed on schists (a), mudstones and sandstones (b), and conglomerates (c). The bold solid lines, solid lines and broken lines correspond, respectively, to the test, validation, and ruled-out soils.

Fig. 2. Soil-moisture characteristic curves (fine-earth sample) for the test soils S1-S4 (solid lines) and a validation soil from G1-G4 (broken lines).

Fig. 3. Relationship between mass wetness and CIELAB lightness in undisturbed core samples of the test soils S1-S4. Measurements taken in wetting and drying branches are shown, respectively, as diamonds and triangles (Model 1). Measurements taken at fixed water potentials (Model 3) are represented by error bars (*SE*).

Fig. 4. Relationship between mass wetness and CIELAB lightness in disturbed fine-earth samples of the test soils S1-S4. Black markers correspond to Model 2 and open markers with error bars (*SE*) to Model 4.

Fig. 5. a) Means and 95% least-significant-difference intervals for soil lightness measured in undisturbed cores of S4 at 19 mass-wetness levels. b) Mass wetness at fixed potentials versus CIELAB lightness in undisturbed core (solid line) and disturbed fine-earth (broken line) from S2.

Fig. 6. Comparison of predicted and measured mass-wetness-data (%) in the validation soils G1-G4. The data encircled correspond to values predicted and measured below permanent wilting point, with available water, and near field capacity. The soil lightness measured in these three wetness ranges (mean ± *SD*) are listed for undisturbed (L*u) and disturbed (L*d) samples.

Figure 1

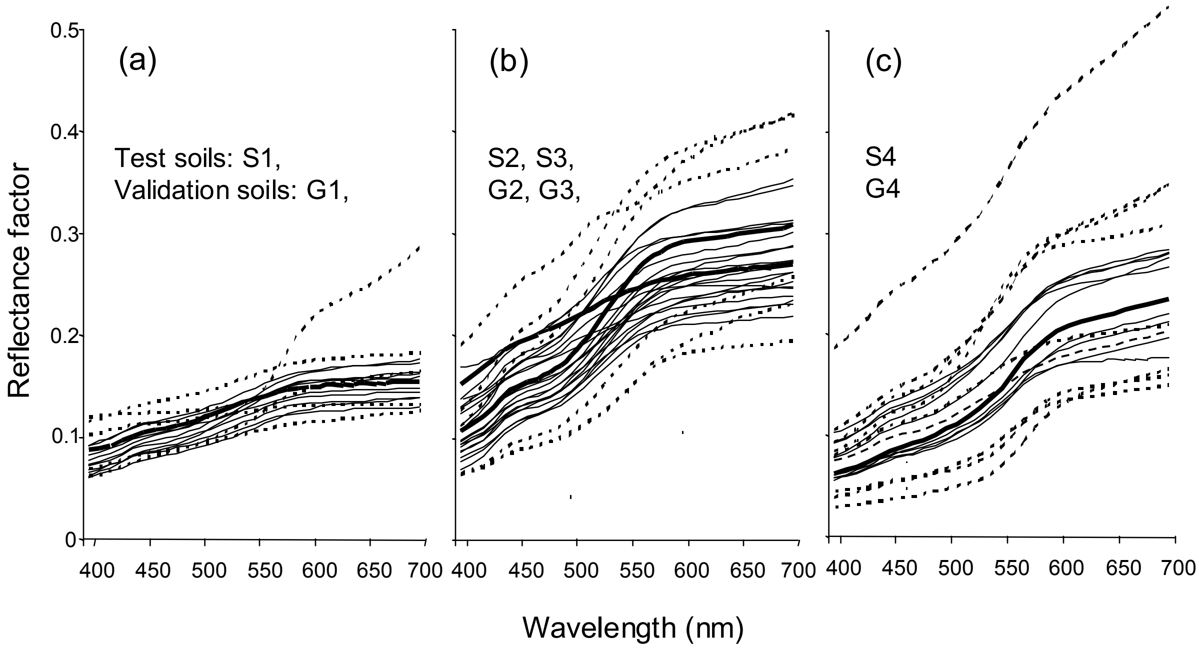
(a)
Test soils: S1,
Validation soils: G1,
(b)
S2, S3,
G2, G3,
(c)
S4
G4
Reflectance factor
0
0.1
0.2
0.3
0.4
0.5
400
450
500
550
600
650
700
Wavelength (nm)

Figure 2

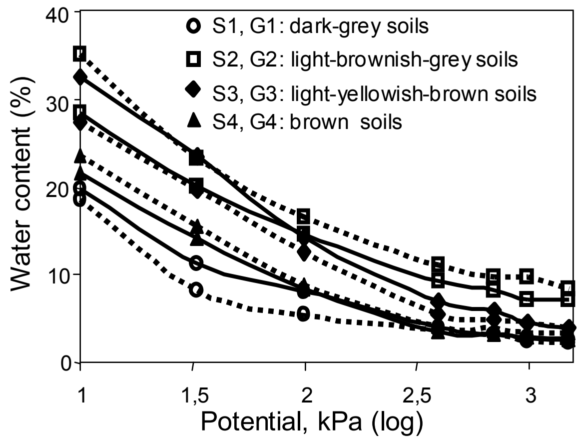

40
30
20
10
0
Water content (%)
1
1,5
2
2,5
3
Potential, kPa (log)
S1, G1: dark-grey soils
S2, G2: light-brownish-grey soils
S3, G3: light-yellowish-brown soils
S4, G4: brown soils

Figure 3

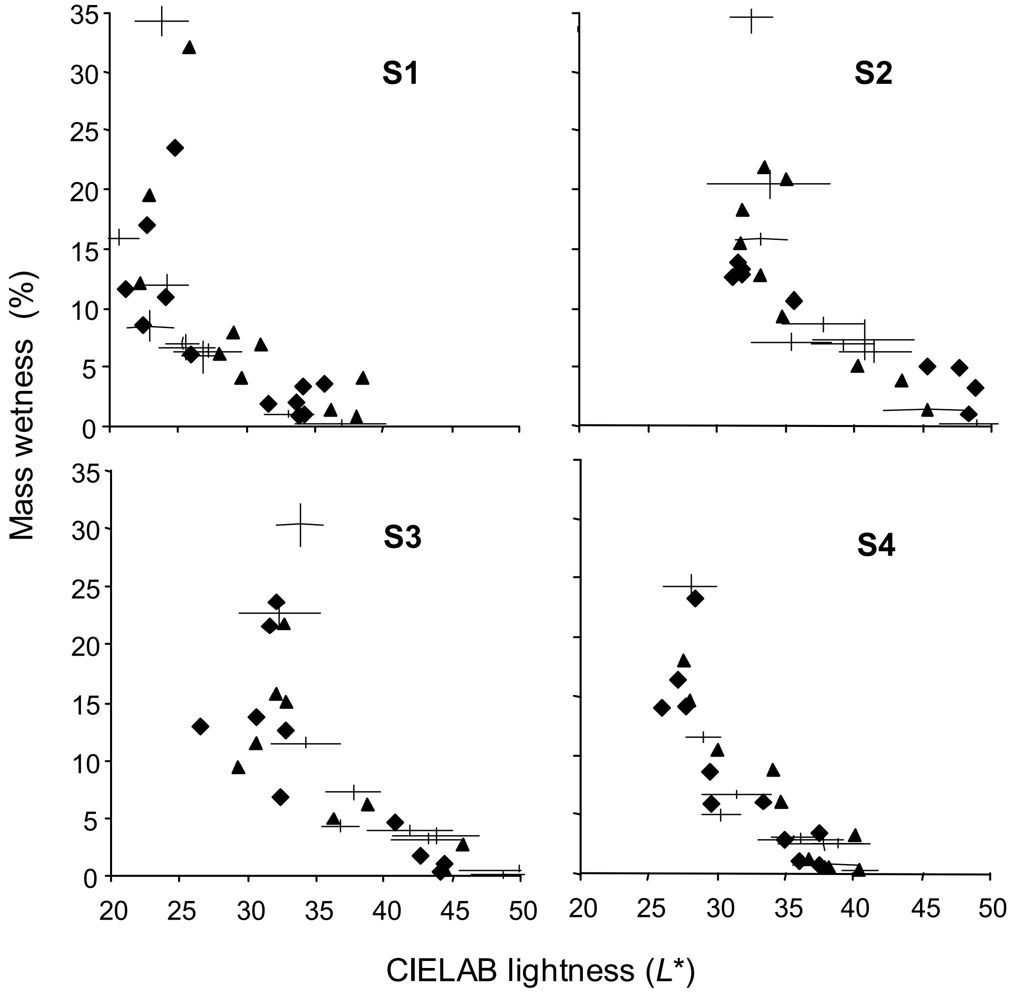

S1
S2
S3
S4
Mass wetness (%)
CIELAB lightness (L*)
35
30
25
20
15
10
5
0
20
25
30
35
40
45
50

Figure 4

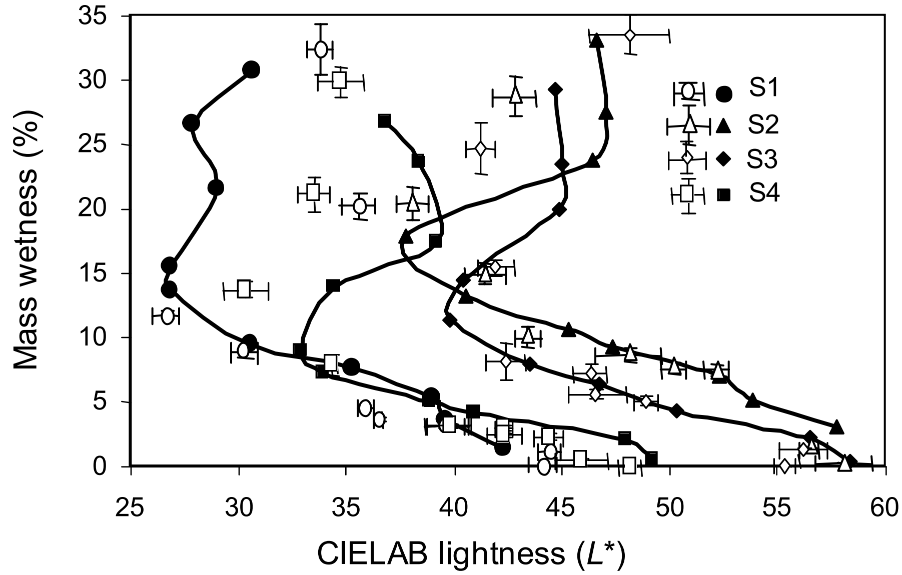

35
30
25
20
15
10
5
0
Mass wetness (%)
25
30
35
40
45
50
55
60
CIELAB lightness (L^*)
S1
S2
S3
S4

Figure 5

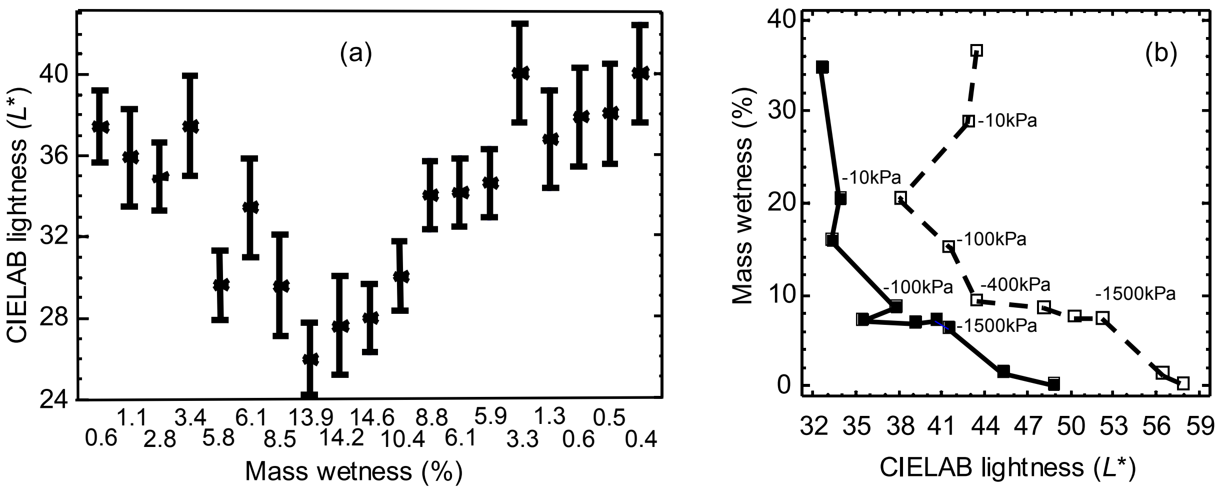
(a)
CIELAB lightness (L^*)
40
36
32
28
24
0.6
1.1
2.8
3.4
5.8
6.1
8.5
13.9
14.2
14.6
10.4
8.8
6.1
5.9
3.3
1.3
0.6
0.5
0.4
Mass wetness (%)
(b)
Mass wetness (%)
40
30
20
10
0
-10kPa
-10kPa
-100kPa
-100kPa
-400kPa
-1500kPa
-1500kPa
32
35
38
41
44
47
50
53
56
59
CIELAB lightness (L^*)

Figure 6

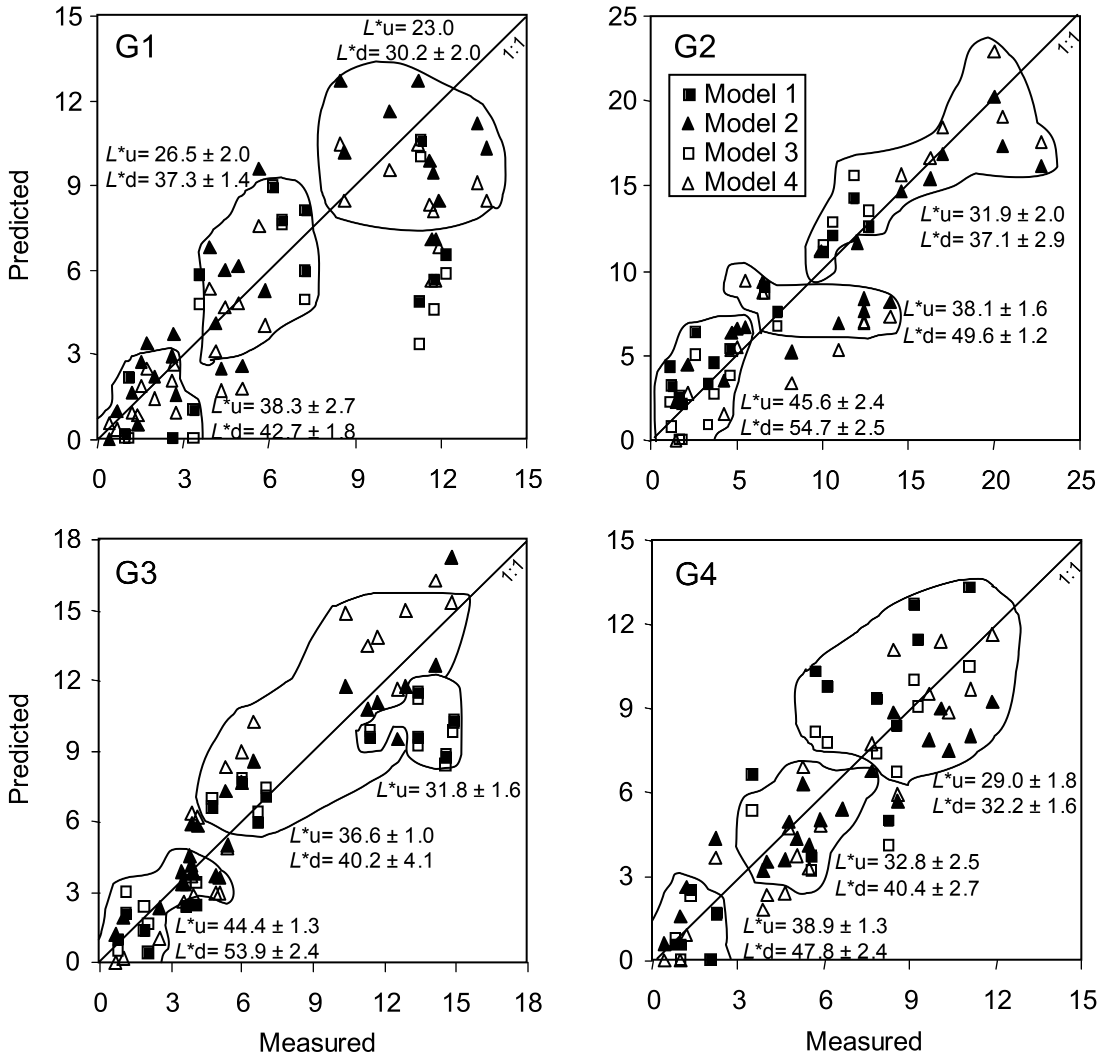
G1
L*u= 23.0
L*d= 30.2 ± 2.0
L*u= 26.5 ± 2.0
L*d= 37.3 ± 1.4
L*u= 38.3 ± 2.7
L*d= 42.7 ± 1.8
G2
Model 1
Model 2
Model 3
Model 4
L*u= 31.9 ± 2.0
L*d= 37.1 ± 2.9
L*u= 38.1 ± 1.6
L*d= 49.6 ± 1.2
L*u= 45.6 ± 2.4
L*d= 54.7 ± 2.5
G3
L*u= 31.8 ± 1.6
L*u= 36.6 ± 1.0
L*d= 40.2 ± 4.1
L*u= 44.4 ± 1.3
L*d= 53.9 ± 2.4
G4
L*u= 29.0 ± 1.8
L*d= 32.2 ± 1.6
L*u= 32.8 ± 2.5
L*d= 40.4 ± 2.7
L*u= 38.9 ± 1.3
L*d= 47.8 ± 2.4
1:1
Predicted
Measured

Table 1

Field description of the A horizons of test soils S1-S4

Sample	Depth cm	Munsell colour [a]		Texture	Structure	Parent material	Classification [b]
		Dry	Moist				
S1	0-20	1.25Y 4.5/1	7.5YR 3/1	Sandy loam	Weak fine granular	Schist	Haplic Regosol (Eutric, Skeletic)
S2	0-12	2.5Y 6/1.5	5Y 4.5/1	Silty loam	Strong thin platy	Mudstone	Haplic Regosol (Calcaric, Hyposalic, Hyperochric)
S3	0-18	2.5Y 6/3	5Y 5/4	Loam	Weak coarse blocky	Sandstone	Haplic Regosol (Calcaric, Hyperochric)
S4	0-6	8.75YR 5/3	10YR 3/4	Loamy sand	Weak fine blocky	Conglomerate	Haplic Regosol (Calcaric)

[a] Visual measurements with Munsell soil colour charts.

[b] IUSS Working Group WRB (2006).

Table 2

Soil properties and mineral composition in fine earth (< 2 mm) of the A horizon of test (S1-S4) and validation (G1-G4) soils

Soil	CIELAB colour (air-dry) h_{ab}	CIELAB colour (air-dry) L*	CIELAB colour (air-dry) C^*_{ab}	Gravel	Sand %	Clay	P_{total}[a] cm^3 cm^{-3}	P_{macro}[a] cm^3 cm^{-3}	Bulk density Mg m^{-3}	OC[a]	Fe_d[a] %	$CO_3^{=}$[a]	EC[a] dS m^{-1}	pH	CEC[a] cmol+kg^{-1}	Mineralogy[b] % M	Q	Ch	Ca
S1	75.7	44.4	7.4	49	68	5	0.48	0.31	1.38	1.0	1.7	0.0	0.2	8.3	4.4	49	17	29	1
S2	85.0	56.5	8.0	15	18	23	0.49	0.21	1.39	0.1	0.7	17.6	2.3	7.8	4.8	60	16	4	15
S3	79.6	56.2	19.9	4	40	18	0.52	0.19	1.31	0.2	0.2	24.9	3.1	8.6	4.8	45	24	3	22
S4	65.6	45.9	20.7	38	83	6	0.45	0.25	1.47	0.5	2.2	2.1	0.3	8.3	5.7	34	58	2	2
G1[c]	75.8	43.1	9.3	43	67	8	0.43	0.27	1.51	1.1	1.0	1.7	0.4	8.2	5.7	47	34	12	2
n=10	(4.9)	(6.2)	(32.1)	(34)	(7)	(30)	(12.8)	(14.9)	(10.3)	(78.1)	(80.0)	(99.4)	(37.5)	(4.8)	(64.5)	(25)	(41)	(58)	(200)
G2[c]	79.8	53.6	13.5	14	37	16	0.48	0.16	1.41	0.4	1.0	10.8	4.4	8.4	7.3	54	22	3	15
n=6	(5.4)	(6.5)	(28.9)	(86)	(32)	(37)	(8.0)	(17.8)	(22.7)	(48.6)	(40.0)	(38.9)	(100)	(6.5)	(49.4)	(16)	(14)	(33)	(30)
G3[c]	76.6	52.9	17.5	28	54	14	0.51	0.26	1.31	0.3	0.9	15.1	1.8	8.5	4.8	39	30	3	23
n=7	(4.4)	(3.5)	(12.9)	(47)	(13)	(39)	(12.6)	(10.6)	(6.5)	(43.3)	(53.0)	(50.9)	(72.2)	(2.8)	(9.3)	(28)	(46)	(99)	(52)
G4[c]	67.7	44.2	18.2	48	70	12	0.49	0.29	1.34	0.8	1.20	4.4	0.5	8.4	7.6	41	43	6	7
n=5	(5.7)	(4.9)	(13.5)	(27)	(14)	(43)	(6.4)	(25.7)	(13.7)	(45.9)	(50.0)	(141)	(37.5)	(9.9)	(36.3)	(20)	(30)	(50)	(128)

[a] P_{total}: Total porosity; P_{macro}: Macroporosity; OC: Organic C; Fe_d: Free Fe extracted with citrate-bicarbonate-dithionite; $CO_3^{=}$: Equivalent $CaCO_3$; EC: Electrical conductivity in the 1:1 extract; CEC: Cation exchange capacity.

[b] Dominant mineral species: M, mica; Q, quartz; Ch, chlorite; Ca, calcite.

[c] Mean values and coefficients of variation (parenthesis).

Table 3

Models for the regression of soil mass wetness (w, %) on CIELAB colour parameters (h_{ab}, L^*, C^*_{ab}) measured in n soil-moisture levels from dry to saturation

Models [a]	R^2	*SEE*	*F*-ratio	w range	Colour range			n
					h_{ab}	L^*	C^*_{ab}	
S1 - Dark grey soil								
(1) $w= 44.85\text{-}4.88C^*_{ab}$	0.62	5.27	33.9	0.8-33.4	67.5-74.7	20.9-38.3	5.2-9.5	22
(2) $w= 72.93\text{-}8.01C^*_{ab}$	0.92	2.86	101.4	1.4-30.6	72.3-76.1	26.8-42.3	5.7-8.6	10
(3) $w= 210.40\text{-}8.29C^*_{ab}\text{-}2.00h_{ab}$	0.82	4.99	21.6	0.0-40.2	66.4-73.0	20.5-36.7	5.3-8.3	10
(4) $w= 542.57\text{-}7.77h_{ab}+1.02L^*$	0.87	3.65	32.1	0.0-32.5	70.7-75.7	26.7-44.4	4.3-8.4	10
S2 - Light brownish grey soil								
(1) $w= 38.61\text{-}0.76L^*$	0.45	3.09	45.1	1.1-21.0	79.5-83.5	31.2-48.9	6.9-8.2	18
(2) $w= 73.70\text{-}6.78C^*_{ab}$	0.39	7.96	6.7	3.3-33.3	80.1-83.5	37.8-57.7	6.7-9.8	10
(3) $w= 178.70\text{-}22.12C^*_{ab}$	0.72	5.43	24.7	0.0-34.7	79.5-83.0	32.5-48.8	6.9-8.1	10
(4) $w= 74.57\text{-}1.29L^*$	0.47	8.62	9.9	0.0-36.7	82.9-85.8	38.0-58.1	7.4-10.3	10
S3 - Light yellowish brown soil								
(1) $w= 40.84\text{-}0.88L^*$	0.60	4.70	24.7	0.3-23.6	70.4-74.3	26.5-45.8	14.4-17.7	19
(2) $w= \text{-}934\text{-}3.68L^*+14.74h_{ab}$	0.86	3.56	29.6	0.4-29.3	74.1-78.1	39.8-58.4	16.4-21.2	10
(3) $w= 1051.49\text{-}13.67h_{ab}\text{-}5.06\ C^*_{ab} +1.16L^*$	0.94	2.40	51.6	0.0-30.4	72.4-75.3	32.3-50.1	14.0-18.6	10
(4) $w= 14.37$	0.00	14.62	0.0	0.0-42.9	77.1-80.9	41.9-56.2	17.3-20.6	10
S4 - Brown soil								
(1) $w= 101.57\text{-}1.15L^*\text{-}0.81h_{ab}$	0.82	2.85	47.6	0.4-23.3	63.6-74.3	25.9-40.4	8.7-16.6	22
(2) $w= 63.77\text{-}2.60C^*_{ab}$	0.53	6.24	11.1	0.7-26.9	62.3-65.3	32.8-49.1	15.8-23.1	10
(3) $w= 49.67\text{-}1.27L^*$	0.60	4.40	14.8	0.0-23.3	64.2-68.5	28.2-40.4	10.4-16.0	10
(4) $w= 424.81\text{-}6.37h_{ab}$	0.84	4.11	46.8	0.0-30.1	63.0-66.9	30.3-48.2	15.0-21.6	10

[a] For each test soil, four models were constructed with: (1) undisturbed soil-core samples, (2) disturbed samples of fine earth, (3) undisturbed soil-core samples at fixed water potentials, and (4) disturbed samples of fine earth at fixed water potentials. R^2: Coefficient of determination adjusted for degrees of freedom, *SEE*: Standard error of estimate, *F*-ratio: F values of analysis of variance test. All models were significant at $P < 0.05$, except (4) for light yellowish brown soil.

Table 4

Models for the regression of soil mass wetness (w, %) on soil lightness (L^*) measured in n moisture levels from dry state to the moisture threshold above which L^* no longer decreases

Model [a]	r	R^2	SEE	F-ratio	w range	L^* range	n
S1 - Dark grey soil							
(1) $w = 23.38-0.60L^*$	- 0.88	0.77	1.89	52.9	0.8-12.1	20.9-38.3	18
(2) $w = 32.48-0.72L^*$	-0.98	0.97	0.85	125.0	1.4-13.6	26.8-42.3	6
(3) $w = 30.54-0.88L^*$	-0.91	0.83	2.14	34.7	0.0-15.8	20.5-36.7	9
(4) $w = 27.47-0.62L^*$	-0.98	0.96	0.82	156.2	0.0-11.7	26.7-44.4	8
S2 – Light brownish grey soil							
(1) $w = 33.14-0.64L^*$	-0.95	0.91	1.51	117.6	1.1-13.7	31.2-48.9	14
(2) $w = 42.46-0.69L^*$	-0.98	0.97	1.01	144.7	3.3-18.1	37.8-57.7	7
(3) $w = 41.07-0.86L^*$	-0.91	0.83	2.13	29.2	0.0-15.8	33.2-48.8	8
(4) $w = 51.78-0.89L^*$	-0.96	0.92	2.00	71.1	0.0-20.3	38.0-58.1	8
S3 – Light yellowish brown soil							
(1) $w = 31.41-0.67L^*$	-0.92	0.85	1.95	69.9	0.3-13.8	26.5-45.8	14
(2) $w = 31.62-0.53L^*$	-0.99	0.97	0.73	140.5	0.4-11.3	39.8-58.4	6
(3) $w = 28.44-0.58L^*$	-0.90	0.80	1.76	24.6	0.0-11.4	34.2-50.1	8
(4) $w = 44.42-0.79L^*$	-0.89	0.80	2.47	20.1	0.0-15.4	41.9-56.2	7
S4 - Brown soil							
(1) $w = 39.85-1.00L^*$	-0.90	0.81	2.17	73.3	0.4-14.6	25.9-40.4	19
(2) $w = 23.03-0.45L^*$	-0.98	0.96	0.68	101.6	0.7-9.13	32.8-49.1	6
(3) $w = 30.60-0.76L^*$	-0.90	0.80	1.65	28.2	0.0-11.3	29.0-40.4	9
(4) $w = 34.44-0.74L^*$	-0.96	0.93	1.32	78.8	0.0-13.9	30.3-48.2	8

[a] For each test soil, four models were constructed with: (1) undisturbed soil-core samples, (2) disturbed samples of fine earth, (3) undisturbed soil-core samples at fixed water potentials, and (4) disturbed samples of fine earth at fixed water potentials. r: Pearson's correlation coefficient, R^2: Coefficient of determination, SEE: Standard error of estimate, F-ratio: F value of analysis of variance test. All models were significant at $P < 0.01$.

Table 5

Differences (absolute values, mean ± standard deviation) between the water content measured in the validation soils G1-G4 and the predicted value from soil lightness by using the Models 1-4 of the respective test soil

Soils	Average of absolute errors				Average of relative errors [a]			
	Model 1	Model 2	Model 3	Model 4	Model 1	Model 2	Model 3	Model 4
G1	2.64±2.21	1.87±1.43	3.05±2.54	1.95±1.96	51.6±32.0	39.1±27.1	56.6±34.9	31.3±18.7
	n = 13	*n* = 29	*n* = 13	*n* = 29	n = 13	*n* = 29	*n* = 13	*n* = 29
G2	1.33±1.12	2.39±1.99	1.61±0.86	2.80±2.26	51.7±74.7	29.9±26.1	46.1±34.9	33.5±28.6
	n = 14	*n* = 20	*n* =14	*n* = 20	n = 14	*n* = 20	*n* = 14	*n* = 20
G3	1.94±1.68	1.17±0.83	1.72±1.82	1.70±1.18	32.1±22.3	25.3±24.4	31.8±37.0	35.0±27.1
	n = 15	*n* = 23	*n* =15	*n* = 23	n = 15	*n* = 23	*n* = 15	*n* = 23
G4	2.03±1.36	1.33±0.92	1.43±1.09	1.27±0.84	45.9±28.9	30.5±29.6	39.4±30.2	32.4±29.1
	n = 15	*n* = 21	*n* = 15	*n* = 21	n =15	*n* = 21	*n* = 15	*n* = 21

[a] Relative errors are calculated with respect to the measured soil-water contents.